

Quantum dots: when nano becomes colourful

Author: Marc Camus Sais

Facultat de Física, Universitat de Barcelona, Diagonal 645, 08028 Barcelona, Spain.

Advisor: Amílcar Labarta Rodríguez - Javier Rodríguez Álvarez

Abstract: The ground state energy of an electron-hole pair confined in a nanometre semiconductor particle (quantum dots) has been studied as a function of size. Three different methods have been used depending on the importance of the quantum confinement. In the regime of weak quantum confinement, the system reduces to a one-body problem, and can be treated as a hydrogen-like atom. In the intermediate regime, the variational method provides an acceptable upper bound of the ground state energy. The trial function used has been properly designed to take into account both the confinement effect and the Coulomb interaction. In the strong confinement regime, the Coulomb interaction can be neglected, and the problem can be solved analytically as a system of two independent particles confined by an infinite "square" potential. The results evidence the strong dependence of the ground state energy on the particle size, which can be applied to tune optical properties at will. Finally, the results have been compared with experimental data.

I. INTRODUCTION

In the 1930s, Herbert Fröhlich was the first to explore the idea that materials properties may depend on macroscopic dimensions due to quantum size effects. Quantum dots (QD), made of small semiconductor particles, are ideal systems for studying these phenomena [1]. Their structure and composition are the same as the bulk materials, but their properties can be tuned with their size. Due to the relevance of QD in optical applications, such as fluorescent labelling and monochromatic light generation [2], the Nobel Prize in Chemistry 2023 was awarded to Moungi G. Bawendi, Louis E. Brus, and Alexei I. Ekimov for the discovery and synthesis of QD.

In a semiconductor, the valence band is the highest energy range which is populated by electrons at zero temperature, while the conduction band is the lowest range of vacant electronic states. The valence band and the conduction band are separated by a band gap, E_g , for which no solution of the Schrödinger equation can be found. An electron from the valence band can absorb energy, being promoted to an excited state in the conduction band, and generating a vacancy in the valence band that can be interpreted as an effective positive charge so-called hole. The electron and the hole can be recombined, emitting a photon with an energy larger or equal to E_g . The fine control of E_g in bulk semiconductors, typically through doping, has allowed for controlled light emission and absorption in a wide range of energies. To describe the kinematics of electrons and holes, the effective mass approximation is typically used, in which effective masses consider the interaction between the electron and the hole with the crystal lattice. Generally, this quantity is defined as a tensor that depends on the curvature of the corresponding energy band. For the sake of simplicity, this work will focus on semiconductors whose energy bands are isotropic and, consequently, m_e and m_h will be scalar quantities. It is useful to define a reduced mass $\mu = m_e m_h / (m_e + m_h)$.

When the electron and the hole are close enough, they

can form a bound system (exciton) through the Coulomb interaction between them. As depicted in Fig. 1 (a), the excitonic states are hydrogen-like and they are found just below the bottom of the conduction band. However, these bound states can easily break down by thermal excitation at room temperature since their energies are very close to the conduction band (see Table I). The ionisation of the excitonic state can be understood as the loss of spatial correlation of the electron-hole pair due to thermal excitation.

In a QD, the ground state (GS) energy of the electron-hole pair can be tuned by changing the QD radius, r_n . This gives rise to a lot of applications involved with display technologies, since the colour of the emitted photon when the electron-hole recombine can be precisely selected. The main focus of this work is to study quantum confinement effects that govern the formation of electron-hole pairs in semiconductor QD. To do so, it is useful to define a unit of length in terms of the Bohr radius, $a_\mu \equiv 4\pi\epsilon\hbar^2/(\mu e^2)$, which is the most probable distance between the hole and the electron in the GS of the exciton. The energy will be expressed in effective Hartree units, $E_\mu \equiv \mu e^4/(4\pi\epsilon\hbar)^2$, which stands for minus twice the GS energy E_{ex} of the exciton in the bulk semiconductor with respect to the bottom of the conduction band. In Table I, a_μ and E_μ for three common semiconductors used to prepare QD can be found.

	m_e/m_0	m_h/m_0	σ	ϵ_r	a_μ (nm)	E_μ (eV)
CdSe	0.13(1)	0.3(1)	2.3(8)	9.56(1)	5.6(9)	0.027(4)
CdS	0.19(1)	0.53(1)	2.79(16)	5.5(1)	2.08(9)	0.126(6)
CuCl	0.4(1)	4.0(5)	10(3)	7.9(1)	1.1(3)	0.16(4)

TABLE I: Reduced effective mass for the electron and the hole, where m_0 is the rest mass of the electron, $\sigma \equiv m_h/m_e$, relative permittivity, Bohr radius, and Hartree energy for CdSe, CdS, and CuCl. Data extracted from [3][4][5].

Depending on r_n , three different regimes can be identified that are associated with weak, intermediate, and

strong quantum confinement. In the weak confinement regime, for $r_n \gtrsim 2a_\mu$, the electron-hole pair is in a hydrogen-like state (exciton), since quantum confinement effects are small and can be treated as a perturbation of the hydrogenic atom. In this regime, the curvature of the wave function increases to fit inside the QD, the GS of the exciton gets closer to the conduction band, and, hence, the bound system weakens as the size of the QD becomes smaller. The critical value of r_n at which the electron and the hole no longer form a bound state due to the kinetic energy becoming larger than the Coulomb energy is the so-called ionization radius, r_i . This is the onset of the intermediate regime where the confinement effects become dominant over Coulomb interaction, the hydrogen-like model is no longer valid, and the system must be treated as a two-interacting particle problem. Finally, once r_n is reduced sufficiently so that the kinetic energy is big enough to neglect the Coulomb interaction, the problem reduces to the case of two particles in a sphere with infinite "square" potential. This corresponds to the strong confinement regime, for which the radius of the QD is about $r_n < 0.5a_\mu$. The energy states when the exciton is ionised can be thought as it is shown in Fig. 1 (b).

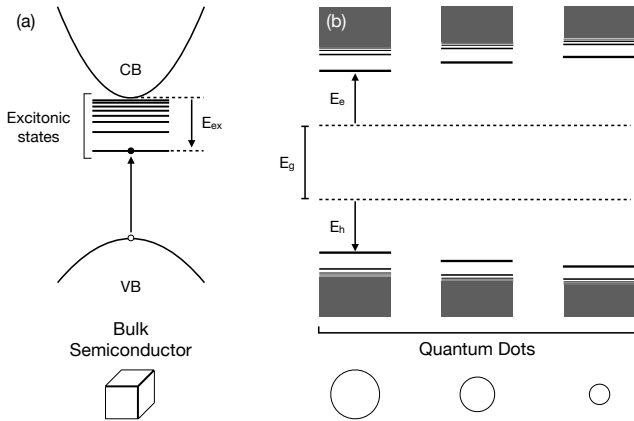


FIG. 1: (a) Valence band, conduction band, and excitonic states in a bulk semiconductor. The separation between the GS of the exciton and the conduction band is not in scale, just for the sake of clarity. (b) Evolution of the energy levels of the electron and the hole as the QD gets smaller in the intermediate and strong confinement regimes.

II. RESULTS AND DISCUSSION

The electron-hole system is described by the Hamiltonian

$$\hat{H} = -\frac{\hbar^2}{2m_e} \vec{\nabla}_{\vec{r}_e}^2 - \frac{\hbar^2}{2m_h} \vec{\nabla}_{\vec{r}_h}^2 - \frac{1}{4\pi\epsilon} \frac{e^2}{|\vec{r}_e - \vec{r}_h|}, \quad (1)$$

where \vec{r}_e and \vec{r}_h are the position vectors of the electron and the hole, respectively. To simplify Eq. (1) it has been used the atomic units $\hbar = e = 1/4\pi\epsilon = 1$. Moreover, the

masses from Eq. (1) are expressed in units of μ

$$\hat{H} = -\frac{\mu}{2m_e} \vec{\nabla}_{\vec{r}_e}^2 - \frac{\mu}{2m_h} \vec{\nabla}_{\vec{r}_h}^2 - \frac{1}{|\vec{r}_e - \vec{r}_h|}. \quad (2)$$

A. Regime of weak quantum confinement

The Hamiltonian in this regime can be turned into a one-body problem changing the variables into the centre of mass position, \vec{R} , and the relative position of the electron and the hole, \vec{r} .

$$\hat{H} = -\frac{1}{2M} \vec{\nabla}_{\vec{R}}^2 - \frac{1}{2} \vec{\nabla}_{\vec{r}}^2 - \frac{1}{r}, \quad (3)$$

where $M = (m_e + m_h)/\mu$ is the total mass of the system in units of the reduced mass, and \vec{r} and \vec{R} are in units of a_μ . This Hamiltonian is separable, so wave functions can be factorised into a plane wave function for the centre of mass and a wave function of an effective particle with mass equal to μ . Due to the spherical symmetry of the problem, the Schrödinger equation is separable in spherical polar coordinates. To solve the radial part, it is convenient to define the reduced radial wave function $P_{nl}(r) \equiv rR_{nl}(r)$ obtaining the following eigenvalues' problem,

$$\left[-\frac{1}{2\mu} \frac{d^2}{dr^2} + V_{eff}(r) \right] P_{nl}(r) = E_{ex} P_{nl}(r), \quad (4)$$

where $V_{eff}(r)$ is the sum of the *opposing* centrifugal energy with the Coulomb potential $V(r)$. Introducing the function $Q_{nl} \equiv \partial_r P_{nl} + lP_{nl}/r$, Eq. (4) can be turned into a system of ordinary differential equations of first order

$$\frac{d\xi}{dr} = A(r)\xi(r), \quad (5)$$

where

$$\xi(r) = \begin{pmatrix} P_{nl}(r) \\ Q_{nl}(r) \end{pmatrix}, \quad A(r) = \begin{pmatrix} l/r & 1 \\ -2(E_{ex} - V) & l/r \end{pmatrix}. \quad (6)$$

This is an integration problem with boundary conditions because it has to be satisfied that $P_{nl}(r_n) = 0$. $P_{10}(r)$ (GS) as a function of r_n was computed using the Hamming method [6]. The calculations were performed using Fortran 90, with a computer code implemented from scratch. The parameter values used in the calculations correspond to the CdSe from Table I. This will also be the case for the calculations in the two other regimes.

Fig. 2 shows $P_{10}(r)$ for three representative QD sizes. For $r_n > 10a_\mu$, $P_{10}(r)$ resembles greatly that of the exciton in a bulk semiconductor. As r_n decreases, the overall curvature of $P_{10}(r)$ increases to satisfy the boundary condition, and so does the kinetic energy. The uncertainty principle, $\Delta x \Delta p \geq \hbar/2$, provides a way of understanding this phenomenon: as the QD is smaller, the uncertainty in the position of the exciton becomes smaller, so

the uncertainty in the momentum is increased, and, consequently, the kinetic energy. For $r_n < 1.835(1) a_\mu$, a hydrogen-like wave function does not fit inside the QD, even for the GS of the system, and $P_{10}(r)$ does not satisfy the boundary conditions since it does not vanish at r_n . At $r_n = 1.835(1) a_\mu$, $E_{ex} = 0$ and the contributions of the kinetic energy and the Coulomb interaction cancel each other. It is worth noting that changing the reference frame to the centre of mass is only valid if the system is bound. Once the system is unbound, the centre of mass has an acceleration and the solutions obtained using this method are meaningless. Moreover, this method underestimates the total kinetic energy of the system since it does not consider the increase in the kinetic energy of the centre of mass as r_n decreases due to confinement effects. Then, the actual value of the ionization radius, r_i , of the exciton should be larger than $1.835(1) a_\mu$.

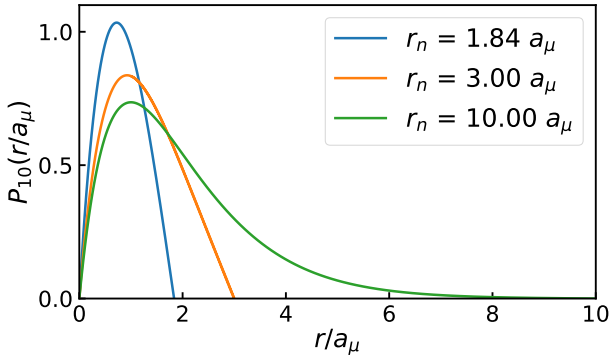


FIG. 2: Reduced radial wave function of the GS for three different QD sizes within the weak quantum confinement regime. Note the increase in overall curvature as the QD size is smaller.

To get a better estimation of r_i the following procedure is proposed. In Fig. 3, it is shown the dependence of the obtained energy on $1/r_n^2$ to show the expected linear behaviour for small values of r_n corresponding to a particle confined in a sphere with infinite "square" potential. For large values of r_n the energy tends asymptotically to -0.5 , the energy of the GS of the exciton in the bulk material expressed in units of E_μ . The intersection between these two limiting behaviours at $r_n = 3.15(5) a_\mu$ provides an estimation of r_i at which the hydrogenic model ceases to be valid because of large contributions of the kinetic energy that ionise the exciton.

B. Intermediate regime

As the size of the QD is smaller, the kinetic energy becomes comparable or even greater than the absolute value of the Coulomb interaction, and the electron-hole pair becomes unbound. Now, the quantum problem is that of a two-particle system. Both particles interact through the Coulomb force, but they are not linked together in a bound state, since the kinetic energy due to the quantum confinement surpasses the Coulomb interaction. This two body problem is described by the general Hamiltonian of

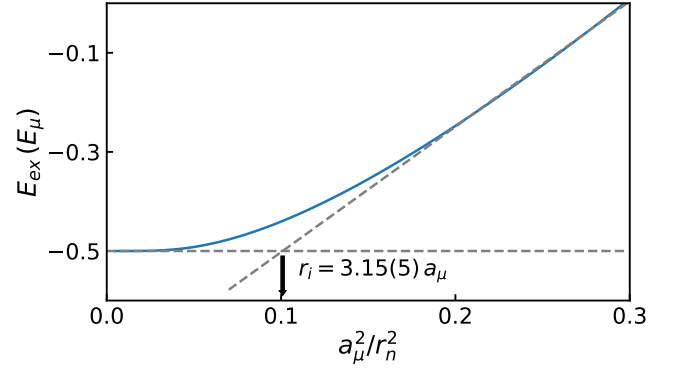


FIG. 3: Dependence of the GS energy of the exciton as the QD gets smaller. The ionization radius is estimated by finding the intersection of the linear regression (dashed line) with $E_{ex} = -0.5 E_\mu$ (horizontal dashed line).

Eq. (2). The problem has still spherical symmetry, since it is going to be found the energy of the GS for $l = 0$. Taking advantage of this symmetry, it is useful to change coordinates: $\{\vec{r}_e, \vec{r}_h\} \rightarrow \{r_e, r_h, r_{eh}\}$, where r_{eh} stands for the distance between the two particles. The calculation of a general element of the Hamiltonian matrix in these coordinates is indicated in Appendix V A. The final result is

$$\begin{aligned} \langle \psi | H | \varphi \rangle = & \iiint_V \frac{\mu}{2m_e} \left\{ \left(\frac{\partial \psi}{\partial r_e} \right) \left(\frac{\partial \varphi}{\partial r_e} \right) + \right. \\ & + \left(\frac{\partial \psi}{\partial r_{eh}} \right) \left(\frac{\partial \varphi}{\partial r_{eh}} \right) + \frac{r_e^2 + r_{eh}^2 - r_h^2}{2r_e r_{eh}} \left[\left(\frac{\partial \psi}{\partial r_e} \right) \left(\frac{\partial \varphi}{\partial r_{eh}} \right) + \right. \\ & + \left. \left. \left(\frac{\partial \psi}{\partial r_{eh}} \right) \left(\frac{\partial \varphi}{\partial r_e} \right) \right] \right\} d\tau + \iiint_V \frac{\mu}{2m_h} \left\{ \left(\frac{\partial \psi}{\partial r_h} \right) \left(\frac{\partial \varphi}{\partial r_h} \right) + \right. \\ & + \left(\frac{\partial \psi}{\partial r_{eh}} \right) \left(\frac{\partial \varphi}{\partial r_{eh}} \right) + \frac{r_h^2 + r_{eh}^2 - r_e^2}{2r_h r_{eh}} \left[\left(\frac{\partial \psi}{\partial r_h} \right) \left(\frac{\partial \varphi}{\partial r_{eh}} \right) + \right. \\ & + \left. \left. \left(\frac{\partial \psi}{\partial r_{eh}} \right) \left(\frac{\partial \varphi}{\partial r_h} \right) \right] \right\} d\tau - \iiint_V \frac{\psi \varphi}{r_{eh}} d\tau. \end{aligned} \quad (7)$$

The volume element results to be $d\tau = 8\pi^2 r_e r_h r_{eh} dr_e dr_h dr_{eh}$, after integration of the whole solid angle, since the operators and the trial functions are all isotropic (see Appendix VB).

The Rayleigh-Ritz variational method [6] provides an acceptable approximation to compute the GS energy of this two-particle problem in the whole range of r_n including the weak and strong confinement regimes because it uses the Hamiltonian in Eq. (2). To choose a good trial function, the following points have been taken into account:

- It has to satisfy the boundary conditions.
- The hydrogen-like solutions for the exciton show an exponentially decaying tail with respect to the variable r . To consider that r for the exciton corresponds to r_{eh} in the two-particle problem.

- The kinetic energy has derivatives with respect to r_e and r_h . \rightarrow Explicit dependences on the coordinates r_e and r_h are necessary.

For convenience, it has been chosen a simple trial function that fulfils all the previous conditions

$$\psi(r_e, r_h, r_{eh}) = \overbrace{\left(1 - \frac{r_e}{r_n}\right)}^{(1)} \overbrace{\left(1 - \frac{r_h}{r_n}\right)}^{(2)} \overbrace{\exp(-\alpha r_{eh})}^{(3)}, \quad (8)$$

where α is a variational parameter to minimise the GS energy. The terms (1) and (2) ensure that the trial function is cancelled when the electron or the hole are at the edges of the QD. Moreover, the dependences on r_e and r_h provide contributions to the kinetic energy as the confinement increases. The term (3) corresponds to the exponentially decaying tail with respect to r_{eh} which stands for the Coulomb correlation between the two particles. The GS energy, E_{eh} , has been computed as the expectation value of the Hamiltonian with this trial function and minimised with respect to α . These calculations have been performed by writing a notebook in the framework of Wolfram Mathematica [7]. In Fig. 4, it is shown the dependence of E_{eh} on r_n minimising the expectation value of the Hamiltonian with respect to α . It is worth mentioning that E_{eh} perfectly converges to $E_{ex} = -0.5 E_\mu$ for large values of r_n as expected. The energy for the GS obtained for the exciton in the Subsection II A predicts lower values than this method, since the model for the confined exciton underestimates the kinetic energy related to the quantum confinement of the two independent particles. To improve the energy estimation of the GS, it has been used the Rayleigh-Ritz variational method with a basis of functions. Suppose a basis of N functions ψ_1, \dots, ψ_N quadratically integrable, which do not have to be linearly independent. A trial function can be obtained as a linear combination of the basis

$$\Psi = \sum_{i=1}^N c_i \psi_i, \quad (9)$$

where c_i are variational parameters that must be appropriately chosen to minimise the energy of the GS. The elements of the basis can be in the form of Hylleraas functions [8] consisting of products of a trial function (that in Eq. (8) in our case) and powers of r_e , r_h , and r_{eh}

$$\Psi(r_e, r_h, r_{eh}) = \sum_{ijk} c_{ijk} \psi r_e^i r_h^j r_{eh}^k. \quad (10)$$

$E_{eh}(r_n)$ has been computed with a basis of 4 functions with $i, j, k = 0, 0, 0; 1, 0, 0; 0, 1, 0; 0, 0, 1$. To perform these calculations, a program has been written in Wolfram Mathematica. It works as follows:

1. For a given α value, it has to be solved a generalised eigenvalue problem

$$\det(H_{nm} - \lambda \Lambda_{nm}), \quad (11)$$

where $H_{nm} \equiv \langle \psi_n | \hat{H} | \psi_m \rangle$ and $\Lambda_{nm} \equiv \langle \psi_n | \psi_m \rangle$.

2. The minimum eigenvalue is the best upper bound for the current value of α .
3. This process is repeated for a range of α . The minimum eigenvalue along this process is the best upper bound for the GS.

As it can be seen in Fig. 4, the results with this basis do not improve significantly the curve obtained using a single trial function. This is because the trial function of Eq. (8) has already most of the features that are relevant in the exact wave function of the GS. It is worth remarking that $r_n = 2.23(1) a_\mu$ at which $E_{eh} = 0$ provides an estimation of r_i which is in agreement with the value obtained in Subsection II A.

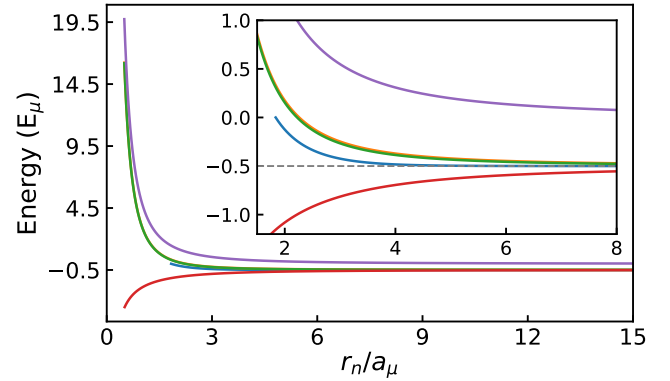


FIG. 4: GS energy as a function of r_n . Energy of the exciton from the weak confinement model (blue curve). Variational method with the trial function of Eq. (8) (orange curve). Variational method with the basis of 4 functions (green curve). Results for the strong confinement model (purple curve). Estimation of the Coulomb interaction between the two particles by subtracting the purple curve from the green curve (red curve). The inset is a zoom of the intermediate regime.

C. Regime of strong quantum confinement

For $r_n \lesssim 0.5 a_\mu$, the results from the variational method are very noisy since they involve calculations with very large numbers as arguments of the exponential functions become smaller. However, in this regime, the energy due to Coulomb interaction is negligible with respect to the kinetic energy of the two particles. Therefore, the problem can be treated as that of two independent particles enclosed in a sphere with infinite "square" potential. The Hamiltonian is still that given in Eq. (2) but without the potential energy due to the Coulomb interaction. Then the eigenstates can be factorised as $\Psi(\vec{r}_e, \vec{r}_h) = \psi(\vec{r}_e)\psi(\vec{r}_h)$, and the problem is analytically solvable (see Appendix V C). The energy of the GS for the electron-hole pair is

$$E_{eh} = E_e - E_h = \frac{1}{2} \left(\frac{\pi}{r_n} \right)^2. \quad (12)$$

As it is shown in Fig. 4, the GS energy calculated by this method connects with the results from the varia-

tional method at approximately $r_n = 0.5 a_\mu$ and provides a simple way to calculate the energy of the system for $r_n < 0.5 a_\mu$, where the numerical errors involved in the calculations of the variational method are too large to obtain reliable results.

III. COMPARISON WITH EXPERIMENTAL DATA

The results from the variational method have been compared with experimental data found in the literature. Fig. 5 shows the energy shift, defined as $E_{shift} = E_{eh} + 0.5 E_\mu$, for different ratios between the electron and hole masses, $\sigma \equiv m_h/m_e$. Since m_e and m_h play symmetric roles in Eq. (2), the results for $\sigma < 1$ are not plotted, as the curves would be identical if σ were defined as $\sigma \equiv m_e/m_h$.

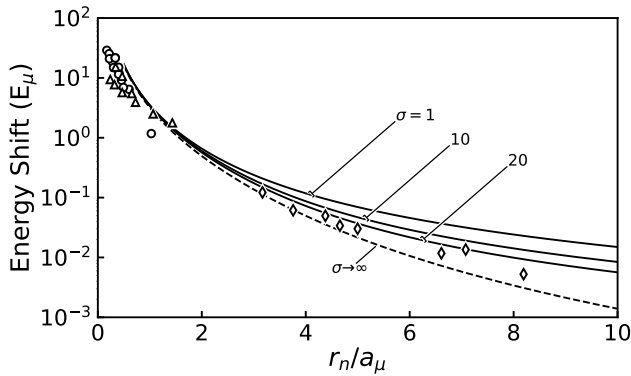


FIG. 5: Energy shift computed for several values of σ represented in a semilogarithmic plot as a function of r_n . Experimental data CdS [4][9] (triangles), CuCl [9] (diamonds), and CdSe [10] (circles). Error bars were not indicated in the original references for the data corresponding to CdSe and CuCl, so they are not drawn in the graph for CdS either for the sake of clarity.

There is a good qualitative agreement between the overall trends of the calculated curves and the experimental data, but not a perfect match with the curve corresponding to the σ value for each set of experimental data (see Table I for values of σ). The experimental points are

generally under the estimated energies as expected, since the variational method gives an upper bound. Moreover, notice that along this work two important approaches have been taken. Firstly, m_e and m_h have always been taken constant and equal to the bulk values as the QD is smaller. This may be a gross approximation for small particles where quantum confinement effects are important and there is always a Coulomb interaction between the electron and the hole. Secondly, confinement inside the QD has been approximated by an infinite "square" potential. In real QD, confinement potentials are finite and the electron and the hole have a certain probability to spread outside the QD. This reduces the kinetic energy related to the quantum confinement, resulting in a lower total energy.

IV. CONCLUSIONS

The variational method provides a good estimation of the GS energy across all three regimes, since the trial function incorporates the essential features. The estimation of the GS energy aligns perfectly with the limits of small r_n and $r_n \rightarrow \infty$, where analytical solutions are known. Furthermore, experimental data are in excellent agreement with the behaviour predicted by the variational method, even though it is not possible to match each set of experimental data with the corresponding curve for the expected σ value.

Acknowledgments

Thanks to my advisors, Amílcar Labarta and Javier Rodríguez, not only for their guidance and patience during this project but also for making it enjoyable and an exceptional experience. Moreover, I would like to extend my gratitude to Francesc Salvat for providing me with some subroutines used in this work. Also, many thanks to my family and my friends for supporting me throughout these years.

-
- [1] The Nobel Committee for Chemistry. Quantum dots – seeds of nanoscience. NobelPrize.org, 2024.
 - [2] Y. Wang, A. Hu. Carbon quantum dots: synthesis, properties and applications. *J. Mater. Chem. C*, 2:6921–6939, 2014.
 - [3] X. Guo, H. Dong, Y. Qiu G. Niu, L. Wang, R. Gao, W. Li. Inorganic halogen ligands in quantum dots: I, Br, Cl and film fabrication through electrophoretic deposition. *Phys. Chem. Chem. Phys.*, 15:19595–19600, 2013.
 - [4] Y. Wang, N. Herron. Quantum size effects on the exciton energy of CdS clusters. *Phys. Rev. B*, 42:7253–7255, 1990.
 - [5] L. Kleinman, K. Mednick. Energy bands and effective masses of CuCl. *Phys. Rev. B*, 20:2487–2490, 1979.
 - [6] F. Salvat. *Mecánica cuántica*. Aula Magna Proyecto Clave McGraw Hill, 2023.
 - [7] Wolfram Research, Inc. Mathematica, Version 14.0. Champaign, IL, 2024.
 - [8] E.A. Hylleraas. Neue Berechnung der Energie des Heliums im Grundzustande, sowie des tiefsten Terms von Ortho-Helium. *Z. Physik*, 54:347–366, 1929.
 - [9] Y. Kayanuma. Quantum-size effects of interacting electrons and holes in semiconductor microcrystals with spherical shape. *Phys. Rev. B*, 38:9797–9805, 1988.
 - [10] U. E. H. Laheld, G. T. Einevoll. Excitons in CdSe quantum dots. *Phys. Rev. B*, 55:5184–5204, 1997.

V. APPENDIX

A. Hamiltonian

The Coulomb potential operator is easily rewritten in these coordinates,

$$\hat{V} = \frac{1}{r_{eh}}. \quad (13)$$

The obtention of the kinetic energy operator is more tedious. The gradient operator in the Cartesian coordinate system is

$$\vec{\nabla} = \vec{e}_x \frac{\partial}{\partial x} + \vec{e}_y \frac{\partial}{\partial y} + \vec{e}_z \frac{\partial}{\partial z}. \quad (14)$$

The variables can be changed into $\{r_e, r_h, r_{eh}, \alpha, \beta, \gamma\}$ (where α, β, γ are the three Euler angles that define the plane spanned by \vec{r}_e and \vec{r}_h) taking into account the spherical symmetry of the space

$$\frac{\partial}{\partial x_e} = \frac{\partial r_e}{\partial x_e} \frac{\partial}{\partial r_e} + \frac{\partial r_h}{\partial x_e} \frac{\partial}{\partial r_h} + \frac{\partial r_{eh}}{\partial x_e} \frac{\partial}{\partial r_{eh}}. \quad (15)$$

Similarly for $\partial_{y_e}, \partial_{z_e}$. Taking into account that $r_e = (x_e^2 + y_e^2 + z_e^2)^{1/2}$, $r_h = (x_h^2 + y_h^2 + z_h^2)^{1/2}$ and $r_{eh} = (x_{eh}^2 + y_{eh}^2 + z_{eh}^2)^{1/2}$, the gradient operator can be expressed as

$$\vec{\nabla}_e = \hat{r}_e \frac{\partial}{\partial r_e} - \hat{r}_{eh} \frac{\partial}{\partial r_{eh}}. \quad (16)$$

The expression for the gradient operator for the holes is analogous to the Eq. (16). To calculate the expectation value of the kinetic energy of two wave functions, the following trick is going to be used. Two first derivatives will be calculated instead of one second derivative

$$\langle \psi | \hat{T} | \varphi \rangle = -\frac{\mu}{2m_e} \langle \psi | \vec{\nabla}_e^2 | \varphi \rangle = \frac{\mu}{2m_e} \langle \vec{\nabla}_e \psi | \vec{\nabla}_e \varphi \rangle. \quad (17)$$

For two given wave functions,

$$\begin{aligned} (\vec{\nabla}_e \psi) \cdot (\vec{\nabla}_e \varphi) &= \left(\frac{\partial \psi}{\partial r_e} \right) \left(\frac{\partial \varphi}{\partial r_e} \right) + \left(\frac{\partial \psi}{\partial r_{eh}} \right) \left(\frac{\partial \varphi}{\partial r_{eh}} \right) + \\ &- \hat{r}_e \cdot \hat{r}_{eh} \left[\left(\frac{\partial \psi}{\partial r_e} \right) \left(\frac{\partial \varphi}{\partial r_{eh}} \right) + \left(\frac{\partial \psi}{\partial r_{eh}} \right) \left(\frac{\partial \varphi}{\partial r_e} \right) \right]. \end{aligned} \quad (18)$$

Since $\vec{r}_e + \vec{r}_{eh} = \vec{r}_h$, it can be obtained

$$\hat{r}_e \cdot \hat{r}_{eh} = \frac{r_h^2 - r_e^2 - r_{eh}^2}{2r_e r_{eh}}. \quad (19)$$

Joining Eq. (18) and Eq. (19), the final expression is obtained

$$\begin{aligned} (\vec{\nabla}_e \psi) \cdot (\vec{\nabla}_e \varphi) &= \left(\frac{\partial \psi}{\partial r_e} \right) \left(\frac{\partial \varphi}{\partial r_e} \right) + \left(\frac{\partial \psi}{\partial r_{eh}} \right) \left(\frac{\partial \varphi}{\partial r_{eh}} \right) + \\ &+ \frac{r_e^2 + r_{eh}^2 - r_h^2}{2r_e r_{eh}} \left[\left(\frac{\partial \psi}{\partial r_e} \right) \left(\frac{\partial \varphi}{\partial r_{eh}} \right) + \left(\frac{\partial \psi}{\partial r_{eh}} \right) \left(\frac{\partial \varphi}{\partial r_e} \right) \right]. \end{aligned} \quad (20)$$

Proceeding analogously for the hole, it can be obtained $(\vec{\nabla}_h \psi) \cdot (\vec{\nabla}_h \varphi)$.

The final expression for a general element of the Hamiltonian matrix is

$$\begin{aligned} \langle \psi | H | \varphi \rangle &= \iiint_V \frac{\mu}{2m_e} \left\{ \left(\frac{\partial \psi}{\partial r_e} \right) \left(\frac{\partial \varphi}{\partial r_e} \right) + \right. \\ &+ \left(\frac{\partial \psi}{\partial r_{eh}} \right) \left(\frac{\partial \varphi}{\partial r_{eh}} \right) + \frac{r_e^2 + r_{eh}^2 - r_h^2}{2r_e r_{eh}} \left[\left(\frac{\partial \psi}{\partial r_e} \right) \left(\frac{\partial \varphi}{\partial r_{eh}} \right) + \right. \\ &+ \left. \left(\frac{\partial \psi}{\partial r_{eh}} \right) \left(\frac{\partial \varphi}{\partial r_e} \right) \right] \Big\} d\tau + \iiint_V \frac{\mu}{2m_h} \left\{ \left(\frac{\partial \psi}{\partial r_h} \right) \left(\frac{\partial \varphi}{\partial r_h} \right) + \right. \\ &+ \left(\frac{\partial \psi}{\partial r_{eh}} \right) \left(\frac{\partial \varphi}{\partial r_{eh}} \right) + \frac{r_h^2 + r_{eh}^2 - r_e^2}{2r_h r_{eh}} \left[\left(\frac{\partial \psi}{\partial r_h} \right) \left(\frac{\partial \varphi}{\partial r_{eh}} \right) + \right. \\ &+ \left. \left(\frac{\partial \psi}{\partial r_{eh}} \right) \left(\frac{\partial \varphi}{\partial r_h} \right) \right] \Big\} d\tau - \iiint_V \frac{\psi \varphi}{r_{eh}} d\tau \end{aligned} \quad (21)$$

B. Volume element

The calculations to obtain the volume element in the coordinates $\{r_e, r_h, r_{eh}\}$ are the following. As a starting point, it is taken the volume element in the coordinates $\{r_e, \theta_e, \phi_e, r_h, \theta_h, \phi_h\}$

$$d\tau = r_e^2 \sin \theta_e dr_e d\theta_e d\phi_e r_h^2 \sin \theta_h dr_h d\theta_h d\phi_h. \quad (22)$$

ϕ_i and one of the θ_i can be integrated, for example θ_e . Moreover, changing the variable, $\theta_h \rightarrow \theta_{eh}$, where θ_{eh} is a relative angle which has the range $0 \leq \theta_{eh} \leq \pi$.

$$d\tau = 8\pi^2 r_e^2 dr_e r_h^2 \sin \theta_{eh} dr_h d\theta_{eh}. \quad (23)$$

Taking into account that $\vec{r}_{eh} = \vec{r}_h - \vec{r}_e$,

$$r_{eh}^2 = r_e^2 + r_h^2 - 2r_e r_h \cos \theta_{eh}. \quad (24)$$

For a given \vec{r}_e and \vec{r}_h which do not change the modulus, if the Eq. (24) is differentiated, it is obtained $r_{eh} dr_{eh} = r_e r_h \sin \theta_{eh}$. Finally, it can be replaced in Eq. (23)

$$d\tau = 8\pi^2 r_e r_h r_{eh} dr_e dr_h dr_{eh}, \quad (25)$$

with the limits $0 \leq r_e \leq r_n$, $0 \leq r_h \leq r_n$, and $|r_e - r_h| \leq r_{eh} \leq r_e + r_h$.

C. Energy states for a particle in a sphere with infinite "square" potential

The Hamiltonian of the electron and the hole in a sphere with infinite "square" potential is

$$-\frac{\mu}{2m_\alpha} \nabla_\alpha^2 \varphi(\vec{r}_\alpha) = E_\alpha \varphi_\alpha(\vec{r}_\alpha), \quad (26)$$

where $\alpha = e, h$ and $\nabla_\alpha^2 = \left[\frac{1}{r_\alpha^2} \partial_{r_\alpha} (r_\alpha^2 \partial_{r_\alpha}) - L^2 / (r_\alpha^2) \right]$. The boundary conditions are $R(r_n) = 0$. The wavefunction can be factorized as $\varphi_\alpha = R_\alpha(r_\alpha) Y_\alpha(\theta_\alpha, \phi_\alpha)$. Introducing this into the Schrödinger equation, it is obtained (without writing α for the sake of simplicity)

$$\underbrace{\frac{1}{Y} L^2 Y}_{(1)} = \underbrace{\frac{2mr^2 E}{\mu} + \frac{1}{R} \frac{\partial}{\partial r} \left(r^2 \frac{\partial R}{\partial r} \right)}_{(2)}. \quad (27)$$

The term (1) only depends on θ, ϕ and the term (2) on r , hence, both terms have to be equal to a constant which will be called $l(l+1)$ for convenience. The equations obtained are

$$L^2 Y = l(l+1) Y, \quad (28)$$

$$\frac{2mr^2 E}{\mu} + \frac{1}{R} \frac{\partial}{\partial r} \left(r^2 \frac{\partial R}{\partial r} \right) = l(l+1). \quad (29)$$

Eq. (28) is an eigenvalue problem whose solutions are the spherical harmonics $Y_{lm}(\theta, \phi)$. To solve Eq. (29), it is useful to rewrite it in the form

$$r^2 \frac{\partial^2 R}{\partial r^2} + 2r \frac{\partial R}{\partial r} + \left(\frac{2mr^2 E}{\mu} - l(l+1) \right) R = 0. \quad (30)$$

Changing the variables $J(\rho) \equiv \sqrt{\rho} R$ and $\rho \equiv kr$ where $k \equiv \sqrt{2mE/\mu}$, it is obtained

$$\rho^2 \frac{\partial^2 J}{\partial \rho^2} + \rho \frac{\partial J}{\partial \rho} [\rho^2 - (l+1/2)^2] J = 0. \quad (31)$$

The solution of this equation is

$$J(\rho) = AJ_\nu(\rho) + BY_\nu(\rho), \quad (32)$$

where J_ν is the Bessel function of the first kind and Y_ν is the Bessel function of the second kind. The Bessel functions of second kind have a singularity in $\rho = 0$, for this reason, $B = 0$. Returning to the variables of the problem, it is obtained

$$R = N j_l(kr), \quad (33)$$

where N is a normalizing constant and j_l is l th order spherical Bessel function. Imposing the boundary condition $R(r_n) = 0$, it is obtained

$$E = \frac{\mu}{2m} \left(\frac{k_{n,l}}{r_n} \right)^2, \quad (34)$$

where $k_{n,l}$ is the n th root of j_l . As the interest of this work is in the GS, it is only needed the first root, which is π . Adding the energy of the hole and the electron, it is finally obtained

$$E = \frac{1}{2} \left(\frac{\pi}{r_n} \right)^2. \quad (35)$$